CCAT-prime: the Design of the Epoch of Reionization Spectrometer Detector Arrays

Yaqiong Li^{a,b}, Jason Austermann^c, James Beall^c, Steve K. Choi^{b,d}, Cody J. Duell^b, Jiansong Gao^c, Zachary B. Huber^b, Johannes Hubmayr^c, Ben Keller^b, Lawrence T. Lin^b, Michael D. Niemack^{b,d}, Thomas Nikola^e, Gordon J. Stacey^d, Joel Ullom^c, Eve M. Vavagiakis^b, Michael Vissers^c, Jordan Wheeler^c, and Bugao Zou^f

^aKavli Institute at Cornell for Nanoscale Science, Cornell University, Ithaca, NY 14853, USA
 ^bDepartment of Physics, Cornell University, Ithaca, NY 14853, USA
 ^cNational Institute of Standards and Technology, Boulder, CO 80305
 ^dDepartment of Astronomy, Cornell University, Ithaca, NY 14853, USA
 ^eCornell Center for Astrophysics and Planetary Science, Cornell University, Ithaca, NY 14853, USA

^fDepartment of Applied and Engineering Physics, Cornell University, Ithaca, NY 14853, USA

ABSTRACT

The Epoch of Reionization Spectrometer (EoR-Spec) is an instrument module that will be deployed in the Prime-Cam receiver on the Fred Young Submillimeter Telescope (FYST), which is a 6m off-axis telescope for the CCAT-prime Facility. FYST is currently being built in the Atacama Desert in Chile at an altitude of 5600 m. With the Fabry-Perot interferometer (FPI), EoR-Spec will measure the 158 μ m [CII] line intensity at redshifts from 3.5 to 8 (420 to 210 GHz), with the lower redshifts tracing star formation and higher redshifts tracing the late stages of reionization. An EoR-Spec module includes three monolithic and monochroic feedhorn-coupled arrays of kinetic inductance detectors (KIDs), two of which are centered at 260 GHz with the other centered at 370 GHz. We present the design and integration process of the EoR-Spec detector array at both bands. The 370 GHz detector array will consist of 3072 detectors and each of the 260 GHz arrays will consist of 1728 detectors. Each of the detector arrays contains an aluminum feedhorn array and is read out by a few pairs of coaxial cables.

Keywords: Cameras, Telescopes, Submillimeter telescopes, Superconducting detector array design, Array packaging

1. INSTRUMENT OVERVIEW

The Fred Young Submillimeter Telescope (FYST) is a 6m off-axis telescope for the CCAT-prime Facility¹ that will be deployed on Cerro Chajnantor in the Atacama Desert in Chile at an altitude of 5600 m. Prime-Cam, which is the main receiver developed for FYST, will be capable of housing seven instrument modules with three detector arrays in each. One of the instrument modules is the Epoch of Reionization Spectrometer (EoR-Spec).² Using a Fabry-Perot interferometer (FPI),³ EoR-Spec will measure the 158um [CII] line intensity at redshifts from 3.5 to 8 (420 to 210 GHz), with the lower redshifts tracing star formation and higher redshifts tracing the late stages of reionization.⁴

The EoR-Spec module will contain three monolithic and monochroic feedhorn-coupled arrays of kinetic inductance detectors (KIDs), which are an emerging technology for the next generation of millimeter and submillimeter telescopes. Two arrays are sensitive to a band centered at 260 GHz, while the third is centered at 370 GHz.

Further author information: (Send correspondence to Y.L.). E-mail: yl3549@cornell.edu

2. EOR-SPEC ARRAY DESIGN

The EoR-Spec array design has evolved from the design of the first 280 GHz detector array for CCAT-prime⁵ and other KID instruments including TOLTEC⁶ and BLAST-TNG.⁷ Fig. 1a shows the array design with the sky side being the top. The 260 GHz (370 GHz) EoR-Spec array will contain 1728 (3072) horn-coupled aluminum KIDs fabricated on a single 6-inch silicon-on-insulator wafer at the National Institute of Standards and Technology (NIST). The 260 GHz (370 GHz) KIDs are split into three (six) groups, and each group of detectors is capacitively coupled to one feedline (shown in Fig. 1c). The wafer stack also contains other silicon layers as shown in Fig. 1b, including a waveguide interface plate (WIP) with ring-shaped choke features on the bottom to guide the photons from the feedhorn array to the detector's antenna, a spacer wafer that holds the WIP and creates an air gap between the chokes and the detectors, and a blank wafer underneath to provide mechanical protection for the delicate backshort structure on the bottom of the detector wafer. The distances between the two opposite edges of WIP and the spacer wafer are 3 mm shorter than that of the detector wafer to allow space for wire bonding.

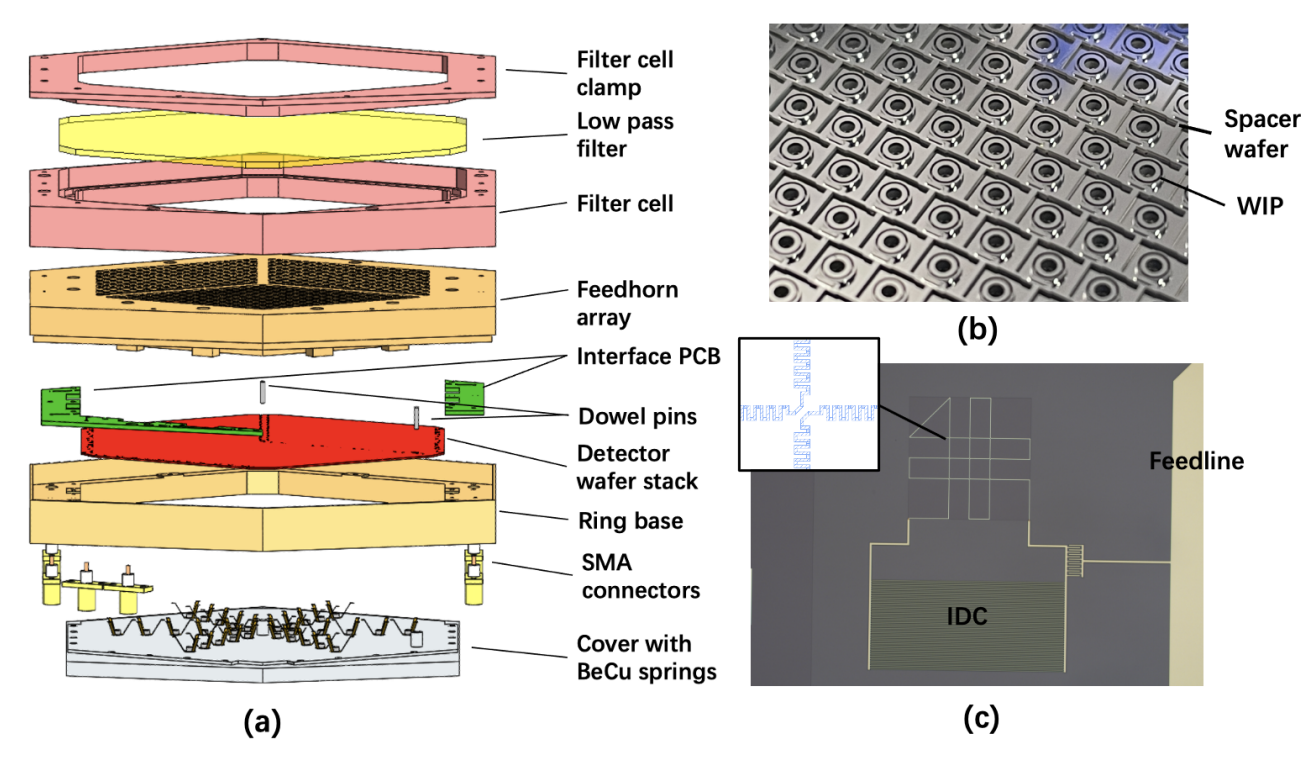


Figure 1. (a) Components of the 260 GHz EoR-Spec KIDs array. (b) Photo of the mechanical WIP wafer and the mechanical spacer wafer fabricated at NIST. (c) Design of a prototype KID for EoR-Spec array from NIST. The prototype aluminum KID consists of an interdigital capacitor (IDC) and an inductive absorber, which is meander-shaped for impedance matching. Photo courtesy of Jordan Wheeler.

The alignment between the detector and the spline-profile feedhorn array is achieved by using two 1.5 mm alignment pins, with one seated in the center hole and the other in the radially-oriented slot to allow for movement due to differential thermal contraction. For vertical alignment, the detector wafer stack will be pushed against the feedhorn array by BeCu tripod springs with a total spring force of ~ 20 N.

Other array components include the low pass filter, the filter cell, the interface PCBs and SMA connectors (as shown in Fig. 1a). With superconducting aluminum wire bonds, the PCBs guide the feedlines to the SMA connectors. An aluminum ring base is designed to house the PCB and SMA connectors. It also serves as a mechanical interface for the feedhorn array and the BeCu spring cover. The detector signal will be read out through NbTi coax cables, amplified by a low-noise-amplifier (fabricated at Arizona State University) at 4 K stage in the cryostat, and eventually received and analyzed by the room temperature hardware.⁸

2.1 Comparison between metal chokes and silicon chokes

Feedhorn Feedhorn PCB Detector wafer Wafer base holder Wefer base holder EoR-Spec detector array WIP Spacer Blank wafer Blank wafer base Temporary holder eventually replaced by spring force (b)

Figure 2. Cross-section sketches of (a) the first 280 GHz array and (b) the EoR-Spec detector array with the sky side being the top.

The main difference between the array design of the EoR-Spec array and the first 280 GHz array⁵ (shown in Fig. 2) is that the ring choke features in the EoR-Spec array are moved into the silicon wafer stack, while for the 280 GHz array the chokes were directly machined on the bottom surface of the feedhorn. The purpose of this change is to avoid the complicated and lengthy machining process of the feedhorn array, which would become practically impossible for the detector arrays at higher frequency bands since the dimension of the choke features scale down with the wavelength. Another advantage is that the optical coupling between the detectors and the feedhorn array for the EoR-Spec array will be improved. For the 280 GHz array, there is a cold 60 μ m gap between the chokes and the detectors to avoid damages to the detector wafer's fabrication layer by possible spurs on the metal feedhorn. For the EoR-Spec array, this air gap is decreased by 10 μ m since the silicon etching process is more precise. However, the current design introduces extra challenges on the integration process, which will be presented in Sec. 3.

3. EOR-SPEC ARRAY INTEGRATION PROCESS

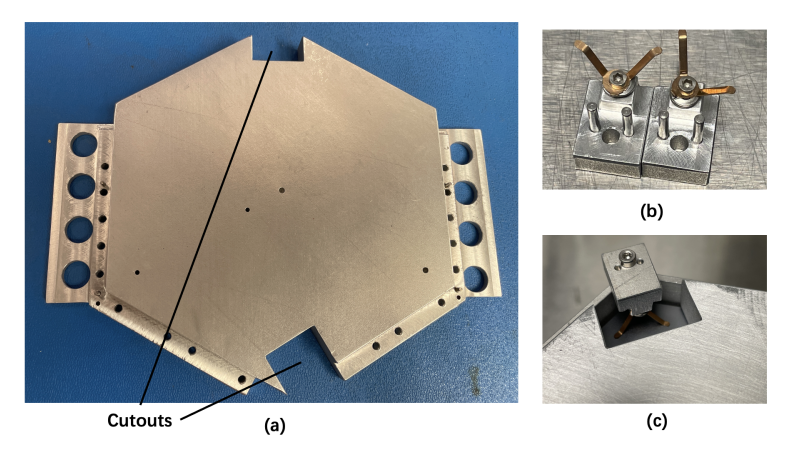


Figure 3. (a) A temporary base designed to hold the detector wafer during wire bonding. (b) Photo of the screw jacks. Alignment pins are added to the screw jacks to make sure that they move straight up when tightening the screws. (c) Photo of a screw jack pushing detector wafer against the feedhorn through the cutouts of the temporary base.

The main challenge of array integration is to place the wire bonds on the feedhorn side of the detector wafer, which will be eventually pushed against the feedhorn array. Hence, we design a temporary base (as shown in Fig. 3) that mounts to the Al ring base from the bottom and temporarily provides a solid substrate for the wafer stack during wire bonding (as shown in Fig. 4). The wafer is aligned to the temporary base by two temporary dowel pins, while the temporary base is also aligned to the ring base by multiple dowel pins. After wire bonding, the feedhorn array is installed to the ring base from the top, leaving an intentional and temporary 100μ gap between the feedhorn and the wafer stack. This gap is to prevent physical damages caused by the feedhorn array on the silicon wafers due to machine tolerances. Similarly to the temporary base, the feedhorn array is aligned to the ring base by dowel pins. Two miniature screw jacks will be installed to the ring base. Through the two cutouts on the temporary base, the springs on the screw jacks will slowly push the detector wafer stack upward by tightening the mounting screws. Pushing the wafer stack against the feedhorn, we flip the entire array upside down and remove the temporary base. After adding alignment pins to the wafers and feedhorn and removing temporary pins, we replace the screw jacks by the BeCu spring cover.

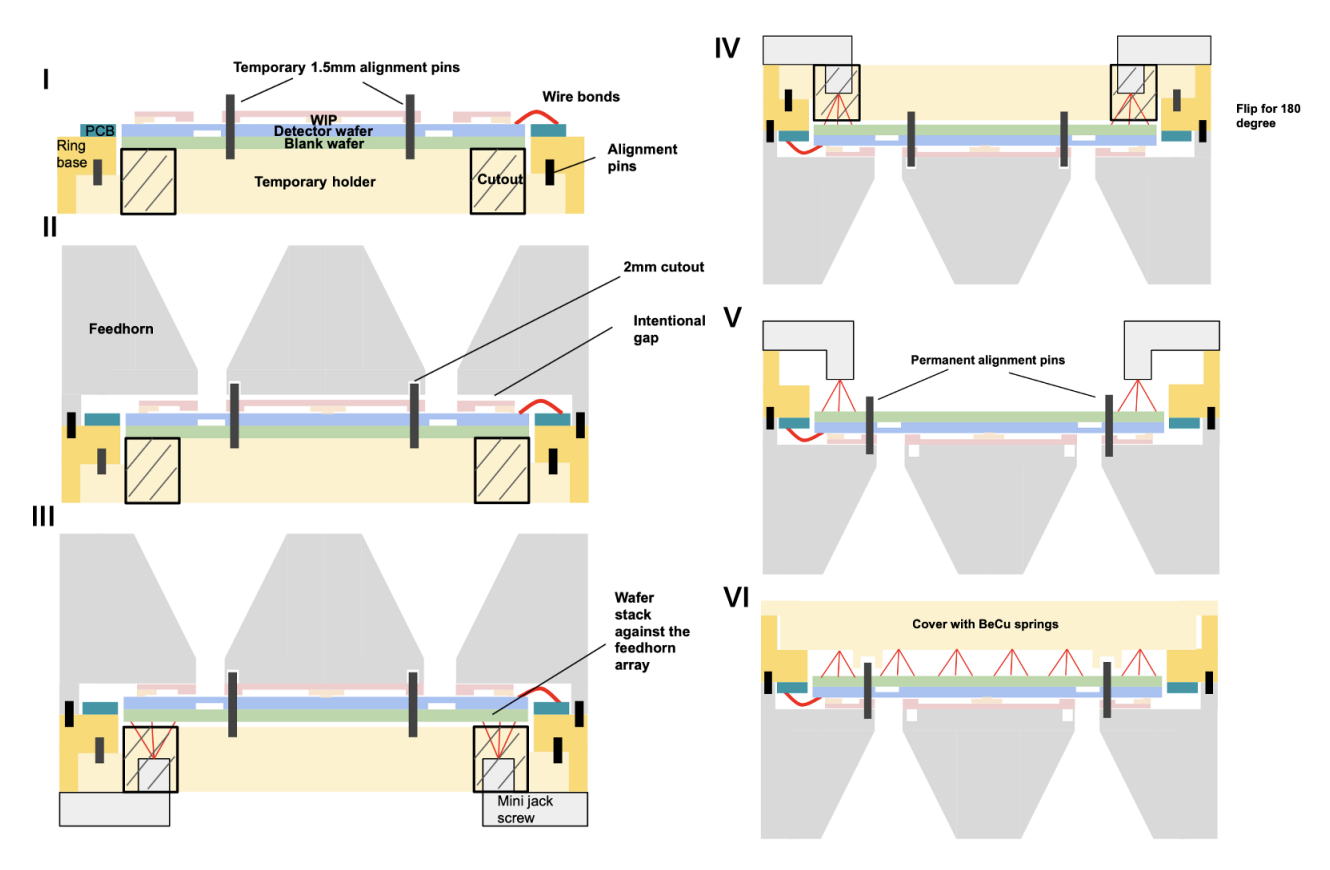


Figure 4. Integration process of the EoR-Spec detector array.

4. MECHANICAL TESTS

A series of cryo-mechanical tests have been conducted with a dummy ring base, feedhorn array, spring cover, and mechanical wafers fabricated at NIST to ensure the integration process can be completed without causing any mechanical damages to the silicon wafers and wire bonds. The integrated mechanical array was also installed to the 4 K stage of a test cryostat to assess the cryogenic robustness. The cryo-mechanical test was successful, showing no damage of any of the wafers and structures, and all wire bonds remained intact.

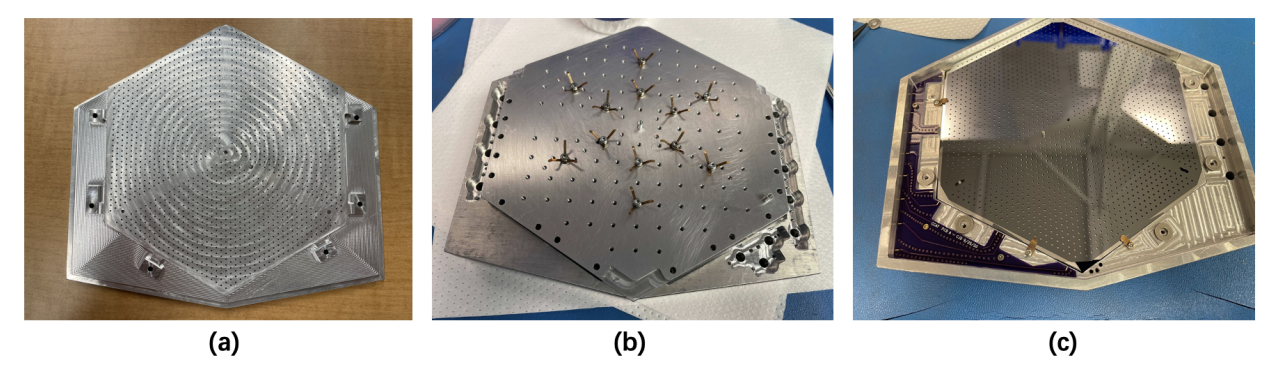


Figure 5. Photos of mechanical test parts, including (a) the dummy feedhorn with cylindrical cutouts, (b) the spring cover and (c) dummy bases with mechanical wafers.

5. CONCLUSION

The current EoR-Spec array design and assembly process are mechanically and cryogenically robust, achieving precise alignment between the detectors and the feedhorn. The design and development work presented here is also important for the design and packaging of future CCAT-prime detector arrays at higher frequency bands.

ACKNOWLEDGMENTS

The CCAT-prime Project, FYST and Prime-Cam instrument have been supported by generous contributions from the Fred M. Young, Jr. Charitable Trust, Cornell University, and the Canada Foundation for Innovation and the Provinces of Ontario, Alberta, and British Columbia. The construction of the FYST telescope was supported by the Großgeräte-Programm of the German Science Foundation (Deutsche Forschungsgemeinschaft, DFG) under grant INST 216/733-1 FUGG, as well as funding from Universität zu Köln, Universität Bonn and the Max Planck Institut für Astrophysik, Garching. The construction of EoR-Spec is supported by NSF grant AST-2009767. YL acknowledges support from the Kavli Institute at Cornell for Nanoscale Science. MDN acknowledges support from NSF grant AST-2117631. ZBH acknowledges support from a NASA Space Technology Graduate Research Opportunities Award. SKC acknowledges support from NSF award AST2001866

REFERENCES

- [1] CCAT-prime Collaboration, "CCAT-prime Collaboration: Science Goals and Forecasts with Prime-Cam on the Fred Young Submillimeter Telescope," (2021).
- [2] Cothard, N.F. et al., "The design of the ccat-prime epoch of reionization spectrometer instrument," *Journal of Low Temperature Physics* **199**, 898 907 (2020).
- [3] Zou, B. et al, "The design and characterization of the silicon mirrors for the Fabry-Perot interferometer in the Epoch of Reionization Spectrometer." SPIE 2022, Paper 12190-148.
- [4] Gong, Y., Cooray, A., Silva, M., Santos, M. G., Bock, J., Bradford, C. M., and Zemcov, M., "INTENSITY MAPPING OF THE [c II] FINE STRUCTURE LINE DURING THE EPOCH OF REIONIZATION," *The Astrophysical Journal* **745**, 49 (dec 2011).
- [5] Duell, C. J., Vavagiakis, E. M., Austermann, J., Chapman, S. C., Choi, S. K., Cothard, N. F., Dober, B., Gallardo, P., Gao, J., Groppi, C., Herter, T. L., Stacey, G. J., Huber, Z., Hubmayr, J., Johnstone, D., Li, Y., Mauskopf, P., McMahon, J., Niemack, M. D., Nikola, T., Rossi, K., Simon, S., Sinclair, A. K., Vissers, M., Wheeler, J., and Zou, B., "CCAT-prime: Designs and status of the first light 280 GHz MKID array and mod-cam receiver," in [Millimeter, Submillimeter, and Far-Infrared Detectors and Instrumentation for Astronomy X], Zmuidzinas, J. and Gao, J.-R., eds., SPIE (dec 2020).

- [6] Austermann, J., Beall, J., Bryan, S. A., Dober, B., Gao, J., Hilton, G., Hubmayr, J., Mauskopf, P., McKenney, C., Simon, S. M., Ullom, J., Vissers, M., and Wilson, G. W., "Large format arrays of kinetic inductance detectors for the TolTEC millimeter-wave imaging polarimeter (Conference Presentation)," in [Millimeter, Submillimeter, and Far-Infrared Detectors and Instrumentation for Astronomy IX], Zmuidzinas, J. and Gao, J.-R., eds., 10708, International Society for Optics and Photonics, SPIE (2018).
- [7] Dober, B., Austermann, J. A., Beall, J. A., Becker, D., Che, G., Cho, H. M., Devlin, M., Duff, S. M., Galitzki, N., Gao, J., Groppi, C., Hilton, G. C., Hubmayr, J., Irwin, K. D., McKenney, C. M., Li, D., Lourie, N., Mauskopf, P., Vissers, M. R., and Wang, Y., "Optical demonstration of THz, dual-polarization sensitive microwave kinetic inductance detectors," *Journal of Low Temperature Physics* 184, 173–179 (dec 2015).
- [8] Sinclair, A.K. et al., "CCAT-prime: RFSoC based Readout for Frequency Multiplexed Kinetic Inductance Detectors." SPIE 2022, Paper 12190-66.